

Moisture buffering capacity of hygroscopic building materials: Experimental facilities and energy impact

Olalekan F. Osanyintola, Carey J. Simonson*

Department of Mechanical Engineering, University of Saskatchewan, 57 Campus Drive, Saskatoon, SK, Canada S7N 5A9

Received 8 September 2005; received in revised form 2 March 2006; accepted 20 March 2006

Abstract

Research into dynamic moisture storage in hygroscopic building materials has renewed interest in the moisture buffering capacity of building materials and shown the potential for these materials to improve indoor humidity, thermal comfort and indoor air quality in buildings. This paper complements previous research by estimating the effect of hygroscopic materials on energy consumptions in buildings. The results show that it may be possible to reduce heating and cooling energy consumption by up to 5% and 30%, respectively, when applying hygroscopic materials with well-controlled HVAC systems. The paper also describes two different experimental facilities that can be used to measure accurately the moisture buffering capacity of hygroscopic building materials. These facilities provide different convective transfer coefficients between the hygroscopic material and ambient air, ranging from natural convection in small, sealed jars to fully developed laminar and turbulent forced convection. The paper presents a numerical model and property data for spruce plywood which will be used in a companion paper [O.F. Osanyintola, P. Talukdar, C.J. Simonson, Effect of initial conditions, boundary conditions and thickness on the moisture buffering capacity of spruce plywood, *Energy and Buildings* (2006), doi:10.1016/j.enbuild.2006.03.024.] to provide additional insight into the design of an experiment to measure the moisture buffering capacity of hygroscopic materials.

© 2006 Elsevier B.V. All rights reserved.

Keywords: Moisture buffering capacity; Energy savings; Experimental facility; Uncertainty; Indoor air quality; Convective transfer coefficients; Spruce plywood

1. Introduction

In recent times, there has been increasing interest to reduce the energy consumption and green house gas emissions associated with the use of mechanical (active) HVAC systems in buildings. In view of this, researchers are investigating the use of passive systems to assist or even eliminate some aspects of these active systems or to control active systems more efficiently. One important aspect is moderating the indoor variations in relative humidity (RH) in buildings because indoor humidity affects warm respiratory comfort [2], skin humidity [3] and perceived indoor air quality [4]. Also, moisture in buildings has been shown to affect the sensible and latent conduction loads [5] and may cause deteriorations in buildings [6]. A recent study [7] included indoor RH as one of the control parameters in a new HVAC control methodology which

provides comfort and air quality near desired levels, while consuming less energy than traditional methodologies. Furthermore, humidity is an important parameter in emergency shelters [8] and supermarkets [9]. The RH is often too high for comfort in shelters that are passively heated by occupants and solar gains even during cold weather, while the RH in supermarkets may vary significantly and is often closely linked to the outdoor temperature. The indoor RH affects the refrigeration load of freezer rooms and display cases and as a result, indoor RH must be included when designing energy recovery for supermarket refrigeration systems [9]. In addition, conservation researchers have shown that a wide variety of artifacts displayed in museums require specific indoor conditions to minimize their deterioration. Yu et al. [10] investigated the use of silica gel as an absorbent to control humidity in museums.

Due to the importance of indoor humidity, several researchers [11–20] have studied the use of various hygroscopic materials to moderate indoor humidity levels. These studies have included laboratory, field and numerical studies and have shown that hygroscopic materials are able to moderate the

DOI of original article: 10.1016/j.enbuild.2006.03.024.

* Corresponding author. Tel.: +1 306 966 5479; fax: +1 306 966 5427.

E-mail address: Carey.Simonson@usask.ca (C.J. Simonson).

Nomenclature

C_p	specific heat capacity at constant pressure (J/(kg K))
D_a	binary diffusion coefficient for water vapor in air (m^2/s)
D_{eff}	effective vapor diffusion coefficient (m^2/s)
D_h	hydraulic diameter (m)
h_a	convective heat transfer coefficient ($W/(m^2 K)$)
h_{fg}	latent heat of vaporization/sorption (J/kg)
h_m	convective mass transfer coefficient (m/s)
H	enthalpy (kJ/kg)
$H_{desired}$	desired indoor enthalpy (kJ/kg)
H_{indoor}	calculated indoor enthalpy (kJ/kg)
k	thermal conductivity ($W/(m K)$)
k_{eff}	effective thermal conductivity ($W/(m K)$)
L	effective thickness of specimen defined as the distance between the surface exposed to ambient air and the impermeable plane in the test specimen (m)
\dot{m}	phase change rate per unit volume ($kg/(m^3 s)$) or mass flow rate (kg/s) in Eq. (11)
MBC	moisture buffering capacity defined as a measure of the mass of moisture that a material can absorb and desorb during a specified humidity cycle per unit exposed surface area (g/m^2)
Nu	Nusselt number
Q	energy transfer (kWh)
Re	Reynolds number of air flow over the specimen
RH	relative humidity (%)
t	time (s)
T	temperature ($^{\circ}C$)
TMT	transient moisture transfer
u	mass of moisture adsorbed per kg of dry spruce plywood (kg/kg)
x	distance from the top of plywood specimen (m)
<i>Greek symbols</i>	
δ	water vapor permeability ($kg/(m s Pa)$)
Δ	difference
ε	volume fraction
ρ	density (kg/m^3)
ρ_0	dry density of the plywood specimen (kg/m^3)
ϕ	relative humidity in fraction
<i>Subscripts</i>	
a	dry air
eff	effective porous media property
g	gas phase (air and water vapor)
i	initial
ℓ	adsorbed phase
s	solid
v	vapor
∞	ambient or free stream property

indoor humidity levels and thus improve the thermal comfort and perceived air quality in buildings, while still providing low energy consumption [20,21]. The impact of hygroscopic materials depends on many factors: the amount and type of materials in a given room, the outdoor climate, the outdoor ventilation rate and the moisture production rate, which also depends on the indoor temperature and RH [22]. During warm and humid outdoor conditions, hygroscopic materials may reduce the peak humidity in a bedroom by up to 35%, 30% and 20% RH when the ventilation rate is 0.1, 0.5 and 1 ach, respectively [11,12]. At a ventilation rate of 0.5 ach, these reductions in peak indoor relative humidity result in a 10–20% reduction in the percent dissatisfied with warm respiratory comfort and a 20–30% reduction in the percent dissatisfied with perceived air quality. The hygroscopic materials used in these studies were wooden paneling, porous wood fiber board and cellulose insulation, but other studies [11–20] have used log panels, cellular concrete, furniture, fabric and other materials. In addition, the porous materials in wall and flooring constructions have been found to be capable of buffering indoor relative humidity and temperature [23]. This paper will extend this research by using published data [11,12] to determine the potential impacts that hygroscopic materials may have on the energy consumption in buildings.

The ability of materials to damp (or buffer) diurnal changes in indoor humidity depends on their active thickness, vapor permeability and moisture storage capacity. The active thickness (or depth to which moisture will penetrate for a given cycle) varies significantly for different materials. For example, Olutimayin and Simonson [24] measured the development of the vapor boundary layer in a bed of cellulose insulation following a step change in ambient humidity and found that the moisture penetration depth was 300 mm, 10 h after a step change in the ambient humidity. They also introduced a moisture property (moisture diffusivity) that is analogous to thermal diffusivity for heat transfer, which takes into account moisture storage. This property can be used to calculate the active thickness of a hygroscopic material. Neglecting moisture storage over predicts the active thickness by a factor of 10 for cellulose insulation.

As noted previously, proper RH control is an important environmental factor not only for humans but also for artifact preservation and passive systems (mostly hygroscopic materials) have some potential to assist in controlling indoor relative humidity. Research indicates that there are many materials that have the capacity to store moisture and buffer indoor humidity changes, but a standard test is needed to compare the ability of various materials to buffer indoor humidity changes [25,26]. Furthermore, two test methods developed to measure the moisture buffering capacity of building materials propose different boundary conditions and material thicknesses [27,28]. The experimental facilities and numerical model presented in this paper support such standard development. A companion paper [1] will apply the facilities and model to investigate the moisture buffering capacity of spruce plywood and document the effect of boundary conditions (convective transfer coefficient and humidity cycle) and specimen thickness on moisture buffering capacity.

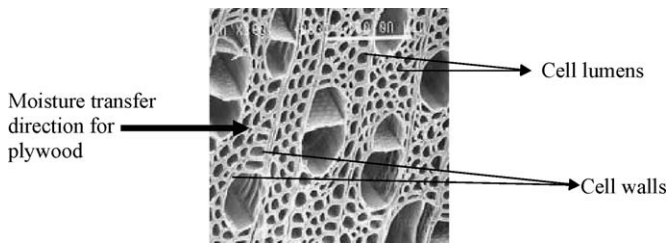


Fig. 1. Scanning electron microscope picture of spruce heartwood showing the cell walls and the cell lumens as well as the main direction of moisture transfer for plywood [28].

2. Plywood material

Plywood is a common building material that gains or releases moisture and heat as the outdoor and indoor conditions change. It is manufactured from different species of peeled wood veneers, such as spruce, oak and pine. These veneers are glued together, layer by layer, to form a panel. Plywood products are produced to be able to withstand extreme weather conditions by using phenolic formaldehyde resin in the gluing process.

All wood products contain moisture, from saturated fresh cut logs to the fairly dry wooden indoor structures and furniture. Moisture in wood is stored as either bound water or free water. Bound water is held within cell walls by bonding forces between water and cellulose molecules. Free water is contained in the cell lumens/cavities and is held by surface tension. A microscopic view of wood is shown in Fig. 1. Since plywood veneers are made by rotating the log and peeling a thin veneer from the log, moisture transfer in the veneer in the direction of the thin dimension is equivalent to moisture transfer in the radial direction of the log. When these veneers are assembled and used in buildings and furniture, the moisture transfer through the exposed surface and into the plywood is equivalent to moisture transfer in the radial direction of the original log. Therefore, the direction of moisture transfer considered in this paper is across the cell walls and lumens (in the radial direction of the original log) as shown in Fig. 1. Because of the rotary peeled veneers, plywood will have more uniform moisture transfer characteristics than raw timber for example, which will have moisture transfer in directions that are both radial and tangential to the wood grains. Therefore, plywood is a good material for the experimental and numerical investigation of moisture buffering capacity.

3. Experimental facilities

In this paper, two facilities are presented that can measure the moisture buffering capacity (MBC) of hygroscopic materials. Each of these facilities creates different convective transfer coefficients between the humid air and the plywood and thus different boundary conditions ranging from natural convection in sealed small jars to fully developed, forced convection air flow (laminar and turbulent) in a small wind tunnel. The size of the sample in the test facilities is also different, but the edges of all plywood pieces are sealed with

aluminium-foil tape to eliminate lateral moisture transfer through the edges. This allows the results to be compared on a per area basis and also represents the application of plywood in practice where moisture transfer through the edges is minimal. In both facilities, the hygroscopic material can be exposed to different humidity cycles, but in this paper, the plywood is exposed to the same 24-h humidity cycle in both facilities—75% RH for 8 h which is followed by a step change to 33% RH for 16 h. This cycle is intended to represent diurnal changes in indoor humidity and is repeated several times. The change in mass is measured gravimetrically with time in each facility.

3.1. Natural convection in 1 L glass jars

This facility tests a small sample of spruce plywood (60 mm × 60 mm × 9 mm) using glass jars containing still air and saturated salt solutions (as shown in Fig. 2). In this facility, both faces of the plywood are exposed to the air in the jar, which creates an impermeable layer at half the thickness of the plywood. The numerical model, presented in Section 4, uses a convection boundary condition at $x = 0$ and an impermeable boundary condition at $x = L$. Therefore, an effective thickness (L) defined as the distance between the surface experiencing convective moisture transfer and the impermeable plane in the test specimen is introduced and will be used throughout this paper. It will be useful when comparing the results of the two facilities in the companion of this paper [1]. In the glass jar facility, the effective thickness (L) for moisture penetration is 4.5 mm from each exposed side.

Prior to testing, the plywood needs to be conditioned to a uniform moisture content. In this paper, the plywood samples are conditioned for a long time (2 months) in the laboratory and the initial moisture content of the wood is 0.028 kg/kg, which corresponds to a relative humidity of about 55%. The plywood sample is then placed in a jar containing a saturated solution and the jars are kept in an environmental chamber that is maintained at 23.3 ± 0.3 °C during the test. The plywood is subjected to a step change in relative humidity by moving it to a jar with a different salt solution. NaCl is used to create the high humidity condition, which creates a humidity of $75.3 \pm 0.1\%$ RH at 23 °C [48] and $MgCl_2$ is used to create the low humidity condition, which creates a humidity of $33.1 \pm 0.2\%$ RH at

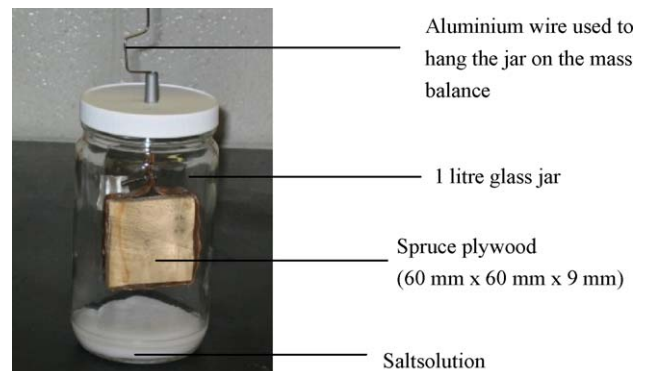


Fig. 2. Picture showing the spruce plywood in a sealed glass jar containing still air and a saturated salt solution.

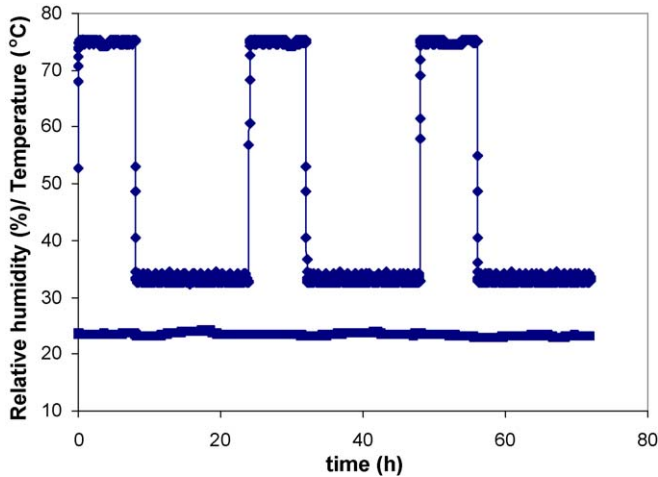


Fig. 3. Measured relative humidity and temperature of the air in the glass jar facility during a typical test, showing the transitions from 75.2 ± 0.8 to $33.3 \pm 0.8\%$ RH at a constant temperature of 23.3 ± 0.3 °C.

23 °C [48]. To determine the actual fluctuation of humidity in the jar, the humidity in the jar was measured during a typical test and the results are presented in Fig. 3. The standard deviation of the humidity is $\pm 0.8\%$ RH at both the high and low humidity conditions. The air inside the jar is not mixed and thus a natural convection boundary layer exists between the vertical surface of the plywood and the air in the jar. The change in mass of the plywood is monitored by periodic weighing using an electronic mass balance with a bias uncertainty of ± 3 mg and a precision uncertainty of ± 0.1 mg. The plywood is not removed from the jar during weighing and the change in mass of the plywood during the humidity cycle can be used to calculate the moisture buffering capacity of spruce plywood. The glass jar facility measures moisture accumulation in spruce plywood, which will be used to calculate the moisture buffering capacity, with a bias uncertainty of ± 0.4 g/m².

In order to determine if the surface area of the salt solution is adequate to maintain a constant RH in the jar especially when

the plywood is first placed in the jar, a temperature/humidity transmitter with uncertainties of ± 0.1 °C and $\pm 1\%$ RH is placed (along with the plywood) in the jar to monitor the temperature and humidity in the jar during a typical test. The transmitter is moved along with the plywood from one jar to another jar during the test and the measured temperature and humidity of the air in the jar are presented in Fig. 3. As can be seen in Fig. 3, the plywood is initially exposed to 75% RH air for 8 h, followed by 33% RH air for 16 h. This cycle is repeated three times. The data in Fig. 3 is recorded every 1 min and therefore it can be seen that it takes about 4 min to realize the change in humidity between 75 and 33% RH. As a comparative test, the temperature/humidity transmitter alone (without the plywood) is moved from one jar to another to check the transient response of the humidity sensor alone. It was found that it takes the sensor less than 1 min to equilibrate with the ambient air in the jar. These tests show that when plywood is first placed in a jar with a salt solution, the plywood has a minor effect on the ambient RH maintained by the salt solution.

3.2. Fully developed air flow in a transient moisture transfer (TMT) facility

In the TMT facility, the experimental apparatus in Fig. 4(a) is used to create fully developed air flow over a bed of hygroscopic material. The convective boundary is controlled by passing air at different flow rates above the material to be tested. In this paper, five pieces of plywood (each with dimensions of 600 mm \times 280 mm \times 9 mm) are placed in a container made of Lexan plastic. The five pieces are held together with nylon screws to reduce air gaps between the pieces (Fig. 4(b)). Other materials could be investigated using different containers. As in the glass jar facility, the four lateral edges of each plywood sample are sealed to minimize lateral moisture transfer. In the TMT facility, there is only one side of the test specimen exposed to moisture transfer. Since the Lexan container is impermeable to moisture transfer, the impermeable plane is at

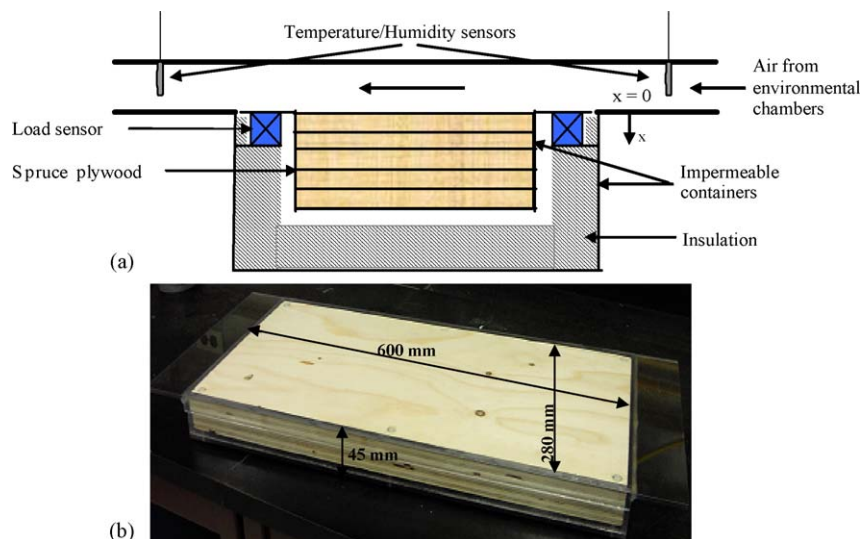


Fig. 4. (a) Schematic of the TMT facility showing spruce plywood and the sensors and (b) picture showing the spruce plywood held together by nylon screws inside the Lexan container.

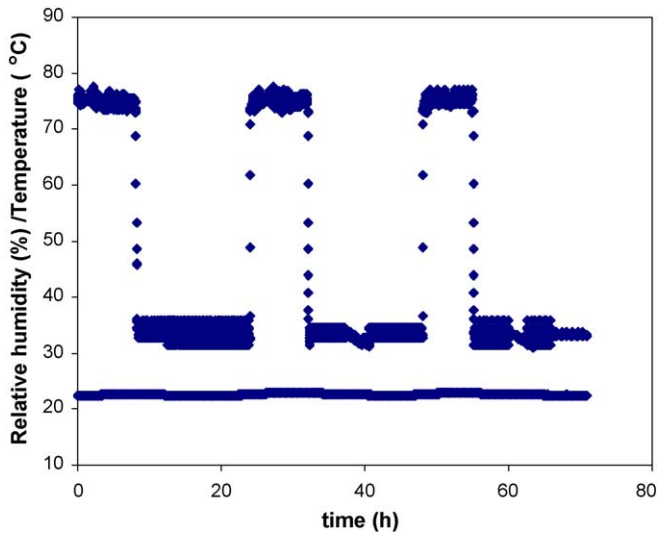


Fig. 5. Plot of relative humidity and temperature of the air entering the TMT facility during a typical test, showing the transition from 75 to 33% RH controlled within $\pm 2\%$ RH and temperature of 22.6°C controlled within $\pm 0.2^\circ\text{C}$.

the bottom of the spruce plywood bed and the effective thickness (L) of the sample is 45 mm. Prior to testing, the plywood samples are conditioned for a long time (4 months) in the laboratory and the initial moisture content of the wood was 0.025 kg/kg, which corresponds to a relative humidity of about 48%.

The air flow is provided by a variable speed vacuum pump, which provides a fully developed air flow over the top of the specimen. The air is drawn from an environmental chamber maintained at a constant temperature ($22.6 \pm 0.2^\circ\text{C}$ in this paper) and a specified humidity (75 and 33% RH in this paper) that can be controlled within $\pm 2\%$ RH. Fig. 5 presents the temperature and humidity measured by the sensor at the inlet of the test section during a typical test. As can be seen in Fig. 5, the plywood is initially exposed to 75% RH air for 8 h, followed by 33% RH air for 16 h. This cycle is repeated three times. The data in Fig. 5 is recorded every 5 min and therefore it can be seen that it takes about 20 min to realize an increase in RH and about 30 min to realize a decrease in RH. It should be noted that this step change is not as rapid nor is the RH control as good as in the glass jar facility presented previously (Fig. 3).

The moisture accumulation/loss in the material under isothermal conditions is measured by four load sensors on which the Lexan container (housing the plywood) is resting (Fig. 4(a)). The load sensors are calibrated with calibration masses and have a bias uncertainty of ± 2 g. Therefore, any change in mass during the test will be continually measured and will be the moisture accumulated or lost by the spruce plywood. These calibrated load sensors allow the TMT facility to measure moisture accumulation in spruce plywood, which will be used to calculate the moisture buffering capacity, with a bias uncertainty of ± 1.1 g/m².

A tapered orifice plate embedded in the supply line downstream of the test section measures the mass flow rate of the air with an accuracy of $\pm 6\%$ according to ISO standard

Table 1

Summary of the convective heat and mass transfer coefficients at different Reynolds numbers in the TMT facility

	Reynolds number, Re		
	1000	2000	4000
Convective heat transfer coefficient, h_a (W/(m ² K))	2.5 ± 0.2	3.5 ± 0.2	8.1 ± 0.4
Convective mass transfer coefficient, h_m ($\times 10^{-3}$ m/s)	2.1 ± 0.2	2.9 ± 0.2	6.7 ± 0.3

5176-1 [29]. The mass flow rate is varied to create different Reynolds numbers (Re) in the air flow channel above the plywood, which results in different convective transfer coefficients between the flowing air and the spruce plywood. The facility is capable of creating air flow Re numbers of up to nearly 10,000. In this paper, Re of 1000, 2000 and 4000, which corresponds to average air velocities of 0.4, 0.8 and 1.6 m/s in the channel above the plywood, will be investigated. The uncertainty in the Re numbers calculated from the measured air flow is $\pm 8\%$ for this facility. A separate test is conducted to determine the convective mass transfer coefficients for these Re numbers. In this test, a tray of water is placed in the TMT facility and air is passed over the free surface of water. As the air with a controlled Re number passes over the test section, water evaporates into the air and the mass of water in the tray decreases, which is recorded by the load sensors. The temperature and relative humidity of the air entering and leaving the test section are measured to determine the vapor density of the air flowing above the water. The temperature of the water is also measured to determine the water vapor density at the surface of the water. From the mass readings and vapor densities, the convective mass transfer coefficient is determined. The measured convective mass transfer coefficient is then used to determine the Sherwood number. With an assumption that the Sherwood number equals the Nusselt number, the convective heat transfer coefficient is determined. The convective heat and mass transfer coefficients determined are shown in Table 1 for the three Reynolds numbers investigated.

4. Numerical model and material properties

Spruce plywood, like any wood material, is a porous material that is made up of solid cell walls and lumens (Fig. 1). The cell walls are irregularly shaped, which makes it extremely difficult to analytically define the boundary between each cell wall and the surrounding fluid. Therefore, local volume averaged equations and properties are used in the model [30]. The assumptions that reflect the experimental conditions and allow the problem to be simplified are as follows: (1) heat and moisture transfer through the spruce plywood is one-dimensional; (2) the transport process within the spruce plywood is pure diffusion of heat and water vapor; (3) air and water vapor behave as ideal gases; (4) the only heat source in the medium is the heat of phase change resulting from the adsorption and desorption of water vapor within spruce plywood ($h_{fg} = 2.5 \times 10^6$ J/kg); (5) the solid and fluid states

are in thermal equilibrium; (6) Knudsen and Fickian diffusion can be combined and thermal diffusion (i.e., Soret effect) can be neglected [31]; and (7) the volume changes (swelling and shrinkage) with changes in humidity are negligible [32].

The resulting conservation equations for mass and energy are listed below [24,32]. The symbols are defined in the nomenclature:

$$\rho_\ell \frac{\partial \varepsilon_\ell}{\partial t} + \dot{m} = 0 \tag{1}$$

$$\frac{\partial(\rho_v \varepsilon_g)}{\partial t} - \dot{m} = \frac{\partial}{\partial x} \left(D_{\text{eff}} \frac{\partial \rho_v}{\partial x} \right) \tag{2}$$

$$\rho C_{p\text{eff}} \frac{\partial T}{\partial t} + \dot{m} h_{fg} = \frac{\partial}{\partial x} \left(k_{\text{eff}} \frac{\partial T}{\partial x} \right) \tag{3}$$

$$\dot{m} = -\rho_0 \frac{\partial u}{\partial t} \tag{4}$$

The boundary conditions for the one-dimensional heat and moisture transfer problem are convective heat and moisture transfer between the spruce plywood and the air above it (Table 1), and an impermeable and adiabatic boundary below the spruce plywood. The initial conditions are constant temperature and relative humidity throughout the spruce plywood and these are determined from the experiment. The relative humidity is calculated based on the initial moisture content and the sorption curve.

4.1. Properties

4.1.1. Sorption isotherm

The sorption isotherm data are measured using the glass jars (Fig. 2) according to the method of Wadso et al. [33] and the data are presented in Fig. 6. The dry mass is obtained by drying in a vented oven at 50 °C until the change in mass between two successive measurements, with a time interval of at least 24 h, is lower than 0.1%. The uncertainty in the mass measurement is ±3 mg and the uncertainty in the moisture content is

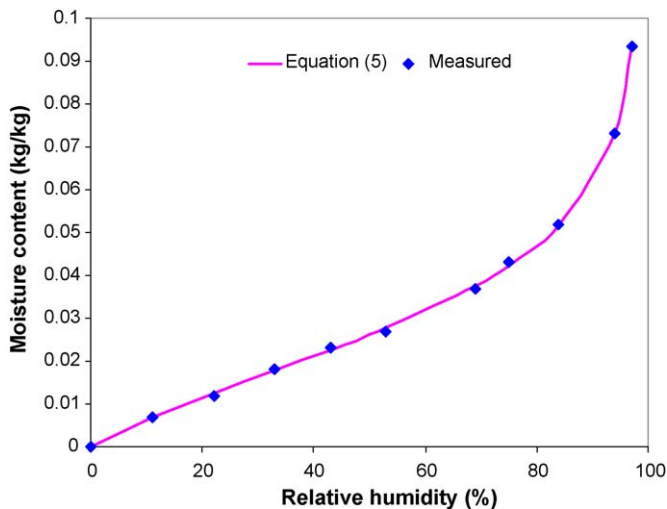


Fig. 6. Sorption isotherm for spruce plywood showing the measured data and the curve fit.

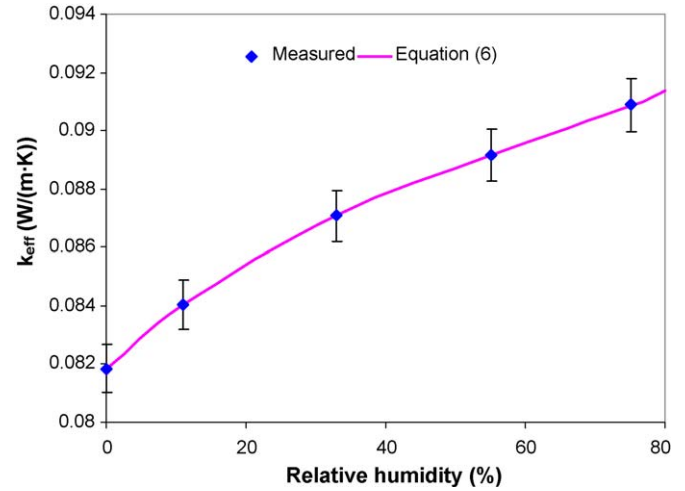


Fig. 7. Effective thermal conductivity curve for spruce plywood showing the measured data with the 95% uncertainty bars and the curve fit.

±0.0001 kg/kg, which corresponds to an uncertainty in moisture content of ±1% at 11% RH and ±0.1% at 97% RH. The experimental data are curved fitted with a continuous polynomial relationship between moisture content (u) and relative humidity (ϕ) in fraction. The polynomial equation for the curve fit is given as

$$u = \frac{a + c\phi + e\phi^2}{1 + b\phi + d\phi^2 + f\phi^3} \tag{5}$$

where $a = 1.0147\text{E}-04$, $b = 0.2339$, $c = 0.06754$, $d = -2.3603$, $e = -0.06574$, $f = 1.1329$. Eq. (5) fits the measured data with $r^2 = 0.999$.

4.1.2. Effective thermal conductivity

The effective thermal conductivity data are measured using a heat flow meter apparatus that measures according to ASTM Standard C518 [34]. The samples are conditioned to the different RH values using saturated salt solutions [48] in order to quantify the change in thermal conductivity with equilibrium RH (Fig. 7). The uncertainty in the measured effective thermal conductivity is ±1%. It should be noted that the thermal conductivity measurements took about 30 min to complete while it took about 14 days to condition the samples to equilibrium, therefore moisture movement during the thermal conductivity test is expected to be minimal. The curve fitted relationship is represented by a polynomial given below:

$$k_{\text{eff}} = a + b\phi + c\phi^2 + d\phi^3 \tag{6}$$

where $a = 0.08185$, $b = 0.02212$, $c = -0.02313$, $d = 0.01291$. Eq. (6) fits the measured data very well as shown in Fig. 7 ($r^2 = 0.999$).

4.1.3. Effective vapor diffusion coefficient

The vapor diffusion coefficient (D_{eff}) can be determined using

$$D_{\text{eff}} = \delta R_v T \tag{7}$$

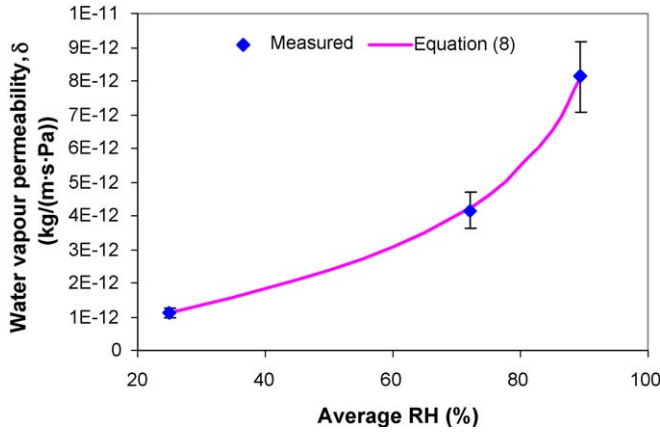


Fig. 8. Water vapor permeability curve for spruce plywood showing the measured data with the 95% uncertainty bars and the curve fit.

where the water vapor permeability (δ) is determined using the cup method [35]. In the dry cup test, CaCl_2 (0% RH) is used in the cup and $\text{Mg}(\text{NO}_3)_2$ (53% RH) is used to condition the surrounding air. The wet cup test uses KNO_3 (94% RH) in the cup and $\text{Mg}(\text{NO}_3)_2$ (53% RH) in the surrounding air. An additional cup measurement is made at high humidities using KNO_3 (94% RH) in the cup and KCl (84% RH) in the surrounding air. The uncertainty in the measured value of δ is $\pm 13\%$. Eq. (8) gives the curve fitted relationship:

$$\delta = \left(a + \frac{b\phi}{\ln\phi} \right)^{0.5} \quad (8)$$

where $a = -2.3573\text{E}-25$, $b = -8.1601\text{E}-24$ (Fig. 8).

4.1.4. Density and specific heat capacity

The equations that quantify the changes in density and specific heat capacity due to moisture adsorption result from the local volume averaging of the governing equations and are

$$\rho = \varepsilon_s \rho_s + \varepsilon_g \rho_g + \varepsilon_\ell \rho_\ell \quad (9)$$

and

$$C_{p\text{eff}} = \frac{\varepsilon_s \rho_s C_{ps} + \varepsilon_\ell \rho_\ell C_{p\ell} + \varepsilon_g \{ (\rho C_p)_a + (\rho C_p)_v \}}{\rho} \quad (10)$$

4.2. Numerical solution

The coupled partial differential equations are discretized using the finite difference method with second order accuracy for the spatial nodes and the implicit scheme for the time derivative. For the spatial nodes at the boundary, the backward or forward scheme is used for the discretization, while the central scheme is used for the central nodes. To provide a stable solution, an under relaxed, Gauss–Seidel iteration method is used and the solution is considered to have converged, when for any time step, the change in any dependent variable (T , ρ_v) is less than 10^{-6} . A sensitivity study showed that a uniform grid size of 0.1 mm and a time step of 30 s provide a numerically accurate solution. Decreasing the grid size to 0.05 mm and the time step to 10 s changes the

moisture buffering capacity by less than 0.1%, but increases the solution time by over five times.

5. Energy impacts of moisture buffering

Hygroscopic materials have the potential to improve indoor climate, comfort and air quality [12,13,15,18,25,36], but the effect of hygroscopic materials on energy consumption has not been studied to the same degree. Therefore, this section attempts to address the question of whether the application of hygroscopic materials can reduce the energy needed to heat, cool and ventilate buildings. The main intent is to identify the magnitude of possible savings and suggest the most promising areas of future work. To accomplish this, results from Simonson et al. [11], which are for a bedroom in a wooden apartment building, will be extrapolated to estimate the potential magnitude of energy savings. This study [11] used hourly weather data from four different cities (Helsinki, Finland; Saint Hubert, Belgium; Holzkirchen, Germany and Trapani, Italy) to calculate the indoor temperature and humidity in a 32.4 m^3 bedroom (floor area of 12 m^2 and internal surface area of 60 m^2) occupied by two adults for 9 h each night (22:00–7:00). The total moisture production was 60 g/h during occupation and the ventilation rate was constant at 0.5 ach. The main hygroscopic materials in the external and internal walls are porous wood fiberboard (11 mm), building paper (0.3 mm) and cellulose insulation (150 mm). All of the internal surfaces are permeable ($5 \times 10^{-9} \text{ kg}/(\text{s m}^2 \text{ Pa})$) except for the floor in the hygroscopic case, while all internal surfaces are impermeable ($5 \times 10^{-12} \text{ kg}/(\text{s m}^2 \text{ Pa})$) in the non-hygroscopic case. These two extreme cases will be used to investigate the potential for hygroscopic materials to affect the energy consumption in buildings. More details of the input data can be found in the literature [11,12]. Even though the simulations of Simonson et al. [11] can be viewed as representing periodic occupation in any building, the extrapolations should be used with caution because the loads, ventilation rate and other factors vary significantly in different buildings.

In this paper, potential savings are divided into “direct” and “indirect” energy savings. Direct savings are savings in the required heating and cooling of a building, while indirect savings are the possible savings that could result due to a lower ventilation rate, a lower indoor temperature in the winter or a higher indoor temperature in the summer.

5.1. Direct energy savings

5.1.1. Heating energy

In the heating season, direct energy savings are possible because moisture accumulation in hygroscopic materials releases 2.5 kJ/kg of moisture, which will decrease the required heating energy. Since humans are an important source of moisture in buildings, this moisture accumulation will occur during occupation. The energy required to heat the 12 m^2 bedroom [11] with one west-facing external wall (150 mm insulation) during the occupied hours (22:00–7:00) is presented in Fig. 9(a) for the hygroscopic and non-hygroscopic cases. In the

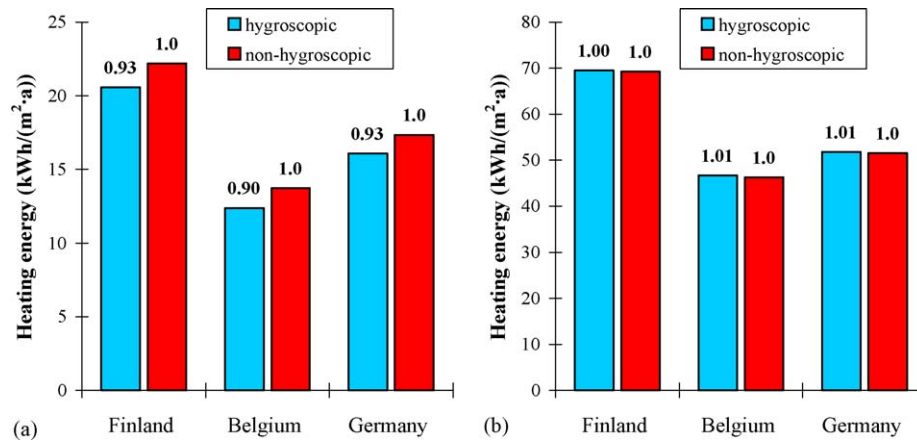


Fig. 9. The heat generated during moisture accumulation in hygroscopic building materials (a) decreases the heating energy consumption during occupation (22:00–7:00), but (b) has a small affect on the total energy consumption during the heating season.

simulations, the heating power is adjusted to keep the bedroom between 20 and 21 °C during the heating season, which was set to be from 1.9 to 31.5 in Finland and from 1.10 to 30.4 in Belgium and Germany. The average indoor temperature was 20.7 °C in Finland and 20.5 °C in Belgium and Germany. Fig. 9(a) shows that the energy consumption during occupation is about 10% lower in the hygroscopic case than in the non-hygroscopic case, which means that moisture accumulation in the building materials during occupation can decrease the needed heating energy. On the other hand, energy is needed to dry this moisture from these materials during unoccupied periods and the net result is that the total energy consumption during the heating season is nearly equal for both cases (Fig. 9(b)). The slightly higher total heating energy consumption in the hygroscopic case is likely due to a slightly higher thermal conductivity due to higher material moisture contents in the hygroscopic case. The results in Fig. 9 show that it may be possible to save heating energy with hygroscopic materials, but a control strategy is required to realize these savings. Such control strategies could be temperature and ventilation set back during unoccupied periods.

5.1.2. Cooling energy

During the cooling season, hygroscopic materials are able to reduce the indoor humidity and consequently reduce the indoor enthalpy [11]. Decreasing the enthalpy of indoor air decreases the energy required to cool the building and also improves the indoor air quality [4,36,37]. The potential for hygroscopic materials to reduce cooling energy consumption can be estimated from the calculated indoor enthalpy. The bedroom studied by Simonson et al. [11] had no cooling, but the energy required to cool the room to a desired enthalpy of 47 kJ/kg (24 °C and 50% RH) can be estimated by the multiplying the area under the curve in Fig. 10 with the ventilation rate (0.5 ach = 4.5 L/s) according to

$$Q = \dot{m}_{\text{ventilation}} \int \Delta H dt \quad (11)$$

where

$$\Delta H = H_{\text{indoor}} - H_{\text{desired}} \quad (12)$$

H_{indoor} is the indoor enthalpy and H_{desired} is the desired indoor enthalpy. Cooling the room is expected to increase the humidity of the indoor air and building materials and will likely increase the moisture transfer from that calculated in [11] because the slope of the sorption curve typically increases with increasing humidity. These effects are neglected here.

The calculated cooling energy and demand are presented in Fig. 11 when the desired indoor enthalpy is 47 kJ/kg, which would result in a percent dissatisfied of 32% if the air was unpolluted [4]. This is comparable to the recommended perceived air quality of 2.5 dp (30% dissatisfied) [38].

Fig. 11 shows that the required cooling energy is quite low for the bedroom because the only internal heat loads are 100 W of lighting for 1 h and two people for 9 h. Nevertheless, the required cooling energy during occupation is lower (from 10% in Italy to 35% in Finland) with hygroscopic materials than with non-hygroscopic materials as shown in Fig. 11(a). The peak cooling demand is also lower (from 10% in Italy to 30% in Finland, Fig. 11(c)) with hygroscopic materials than with non-hygroscopic materials. Similarly as was discussed with the heating energy savings, a control strategy is needed to realize these savings because they represent the energy consumption and demand during occupied hours.

Fig. 11(b) shows that the savings in cooling energy consumption for all hours during the year are lower than during occupation which is similar to the findings of Fairey and Kerestecioglu [39]. Simulation results [39] show that if a building is continuously conditioned regardless of occupation, the cooling energy savings due to hygroscopic mass are in the order of 5% (for the month of July in Atlanta, GA), but if ventilation and cooling are controlled according to occupation greater savings can be realized. It is expected that a control strategy to optimize the benefits of hygroscopic mass would be similar to that recommended to optimize the benefits of thermal mass for the cooling of buildings (e.g. [40–42]). Peak cooling loads can be reduced by as much as 50% by precooling the building mass during unoccupied periods [41], but such savings can be overestimated if the moisture adsorbed in the building structure and furnishings during unoccupied periods is not

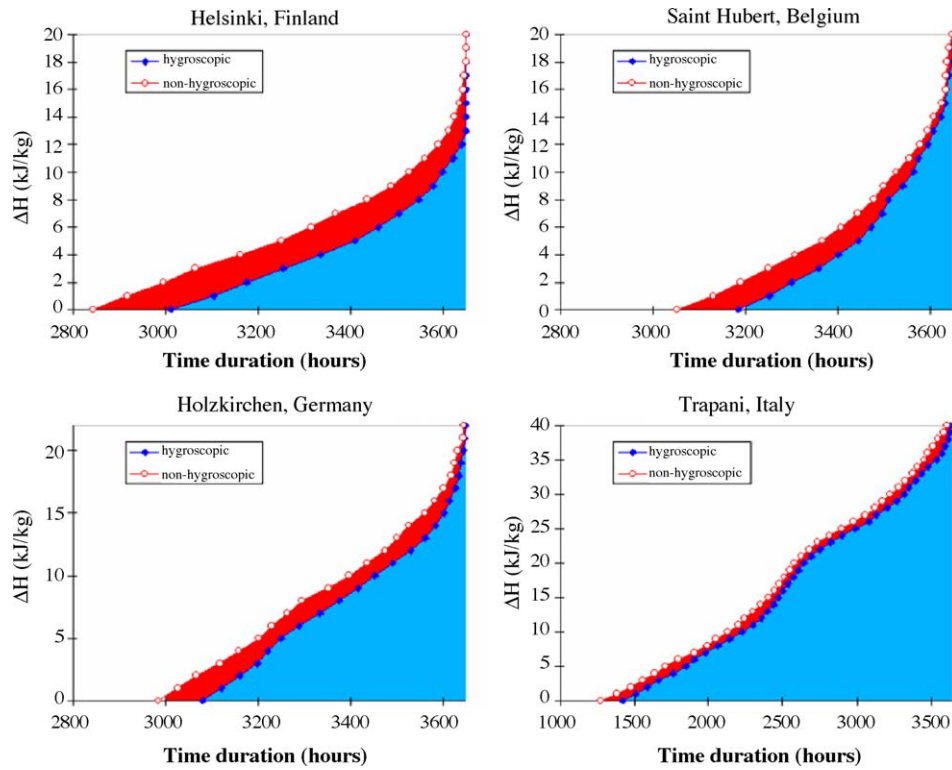


Fig. 10. Frequency distribution of the difference between indoor enthalpy and an enthalpy of 47 kJ/kg during occupied hours. The shaded regions are proportional to the energy required to cool the room to 24 °C and 50% RH (47 kJ/kg).

included [39]. Nevertheless, it is not unreasonable to expect peak cooling load reductions of 10–30% when hygroscopic materials are applied, as shown in Fig. 11(c). This could have a large impact on the size, cost and efficiency of cooling equipment in buildings.

5.1.3. Summary of direct savings

Fig. 12 summarizes the magnitude of the potential savings of heating and cooling energy considering the occupied hours and all hours. In the case including only occupied hours, it is assumed that the HVAC control system is optimized to take advantage of the lower heating and cooling loads during

occupation. The relative heating/cooling energy savings are relative to the total heating/cooling energy consumption (i.e., including both occupied and unoccupied hours) and are therefore lower than the relative savings presented previously.

5.2. Indirect energy savings

The main purpose of conditioning buildings it to provide an indoor environment that is comfortable and an indoor air quality that is acceptable, where temperature, humidity and ventilation (among other factors) affect comfort and air quality [2–4,43]. Therefore, since hygroscopic materials can improve

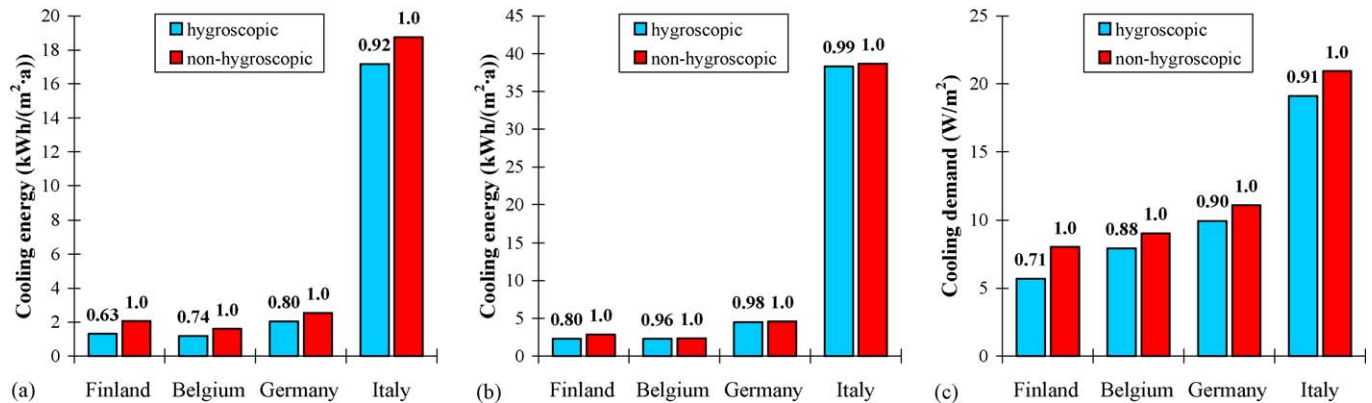


Fig. 11. Cooling energy required to cool the bedroom to an enthalpy of 47 kJ/kg (24 °C and 50% RH) during (a) occupation and (b) all hours, and (c) cooling demand during occupation.

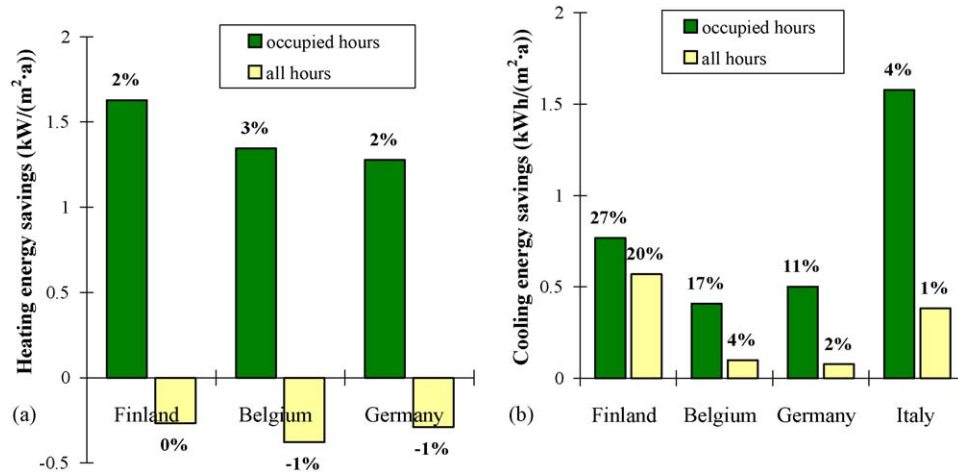


Fig. 12. Potential direct (a) heating and (b) cooling energy savings when applying hygroscopic materials. The percent savings are relative to the total heating or cooling energies.

indoor humidity conditions, it may be possible to alter the temperature and outdoor ventilation rate of buildings that use hygroscopic materials and still provide a similar comfort and indoor air quality as in buildings without hygroscopic materials [12].

5.2.1. Reducing outdoor ventilation

Research has quantified the effect of humidity on perceived air quality and warm respiratory comfort using laboratory experiments [2,4]. In addition, these findings have been confirmed in a field study where it was found that the perceived indoor air quality was moderately better at a ventilation rate of 3.5 L/s per person and an indoor enthalpy of 35 kJ/kg (20 °C/40% RH) than at a ventilation rate of 10 L/s per person and an indoor enthalpy of 45 kJ/kg (23 °C/50% RH) [37]. Therefore, the perceived indoor air quality will be similar if the ventilation is reduced by 75% and the indoor enthalpy decreased by 10 kJ/kg. Since the average indoor enthalpy is about 2 kJ/kg (1.9 kJ/kg in Finland and Belgium, 1.7 kJ/kg in Germany and 1.5 kJ/kg in Italy) lower during occupation in the hygroscopic case than in the non-hygroscopic case [11], the ventilation rate in buildings with hygroscopic materials could possibly be reduced by 15% (i.e., 2 kJ/kg (75%/10 kJ/kg)) and

still provide a comparable IAQ. Simonson et al. [12] found that even larger ventilation reductions were possible, ranging from 20% to 90% depending on the criteria selected. Even though more research is needed before ventilation reductions can be safely brought into practice, Fig. 13 presents the savings that could result with a modest estimation of a 15% reduction in ventilation rate. Here it is important to note that decreasing the ventilation rate is expected to have a greater effect on IAQ as the ventilation rate decreases [44]. Meanwhile, decreasing the ventilation rate is expected to have a smaller effect on energy consumption as the ventilation rate decreases.

Reducing the ventilation rate by 15% would have a significant impact on the energy consumption in Finland and could save an estimated 3 TWh/a of heating energy and 0.6 TWh/a of electricity (Fig. 13(a)). These savings are based on the estimated heating and electricity consumption due to ventilation (21 and 4 TWh/a, respectively) presented by Seppänen [45].

In a case study in Austin, Texas, it was found that reducing the outdoor ventilation rate increased comfort and reduced the measured energy consumption in a 9200 m² office building [46]. To improve the indoor air quality in the building, the outdoor ventilation rate was reduced by 86% (from 74 to 10 L/s

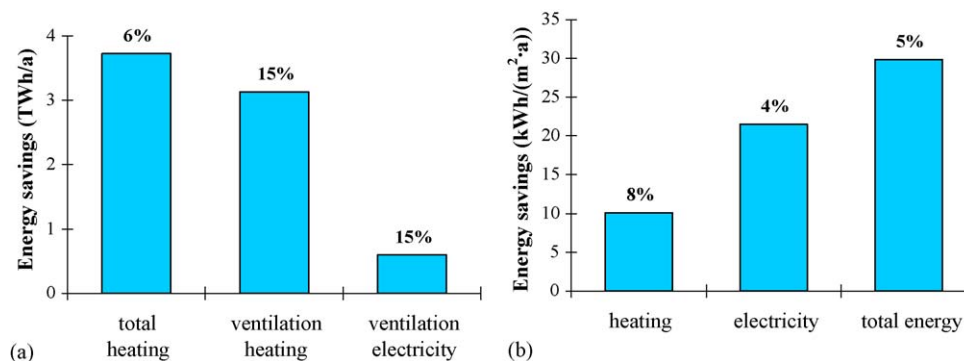


Fig. 13. Possible energy savings in (a) Finnish buildings and (b) an office building in Austin, Texas due to reducing the ventilation rate by 15%.

per person). Decreasing the ventilation rate, decreased the peak indoor relative humidity from 70% to 55% and resulted in a significant improvement in comfort conditions during the summer. In addition to improving comfort, the reduced ventilation rate decreased heating energy use by 48%, electricity use by 21% and total energy use by 27%. Assuming that the decrease in energy use is proportional to the decrease in ventilation rate, a 15% reduction in ventilation rate would reduce the heating energy consumption by 8% and the total energy consumption by 5% (Fig. 13(b)). It is interesting to note that the percent savings in heating energy are similar in Finland and in Texas.

Woloszyn et al. [47] present the numerical analysis of a two-bedroom apartment (140 m³, 60 m²) for one evening (19:00–0:00) in a mild humid climate using the mean January climate of Macon, France. Macon is in east-central France and the average outdoor conditions during the simulation were 3 °C and 93% RH (4.4 g/kg). Woloszyn et al. [47] compared the indoor humidity and energy consumption of the apartment for two cases. One case is where the moisture buffering capacity of the structure and furnishings is included in the simulation and the other case is where the moisture buffering capacity is neglected. The apartment had a mechanical ventilation system and a ventilation rate that varies between 0.12 and 0.7 ach depending on the indoor relative humidity. The simulation results show that the indoor humidity in the kitchen and living room is over 15% RH greater in the non-hygroscopic case than in the hygroscopic case, even though the average ventilation rate is about 10% higher in the non-hygroscopic case than in the hygroscopic case. The total energy consumption during the 6 h period is 45% higher in the non-hygroscopic case than in the hygroscopic case. New ventilation units that control the ventilation rate based on measured humidity and CO₂ could result in additional savings for buildings with hygroscopic materials.

5.2.2. Reducing indoor temperature in the winter

Since the indoor humidity during occupation is reduced when applying hygroscopic materials, the indoor temperature can be reduced and yet result in the same indoor relative humidity. Here it is important to note that relative humidity is

not an important comfort parameter at low temperatures, but has a strong effect on the risk of condensation and mould growth during the heating season [44]. The average indoor temperature in the hygroscopic and non-hygroscopic cases of Simonson et al. [11] are nearly identical (less than 0.2 °C difference). On the other hand, the indoor temperature in the hygroscopic case can be reduced by an average of 1.6 °C in Finland and Belgium and 1.5 °C in Germany, while maintaining the same indoor relative humidity during the occupied hours of the heating season. The potential energy savings due to a reduced indoor temperature are estimated by multiplying the ratio of the temperature reduction (1.5 or 1.6 °C) to the average temperature difference between indoors and outdoors by the heating energy used during occupation. Since the average temperature difference between indoors and outdoors during the occupied hours of the heating season are 21.6, 18.9 and 21.3 °C in Finland, Belgium and Germany, the estimated heating energy savings due to reducing the indoor temperature are 2% of the total heating energy (7–9% of the heating during occupation) as shown in Fig. 14(a).

5.2.3. Increasing indoor temperature in the summer

In the summer, the perceived air quality (PAQ) and warm respiratory comfort during occupation may be significantly poorer in a building with non-hygroscopic materials than in a building with hygroscopic materials [36]. As a result, it is possible to allow the indoor temperature in a building with hygroscopic materials to be higher than in a building with non-hygroscopic materials and still have comparable indoor comfort and air quality. Increasing the indoor temperatures will reduce the energy needed for cooling the building during warm weather. The results of Simonson et al. [11] show that the indoor temperature can be increased by about 1 °C in a hygroscopic building and yet provide similar conditions of warm respiratory comfort. Similarly, a hygroscopic building can have up to 2 °C higher indoor temperature than a non-hygroscopic building and still have similar perceived indoor air quality. The energy savings that could result from such a temperature change are estimated by changing H_{desired} in Eq. (12) and the results are in Fig. 14(b).

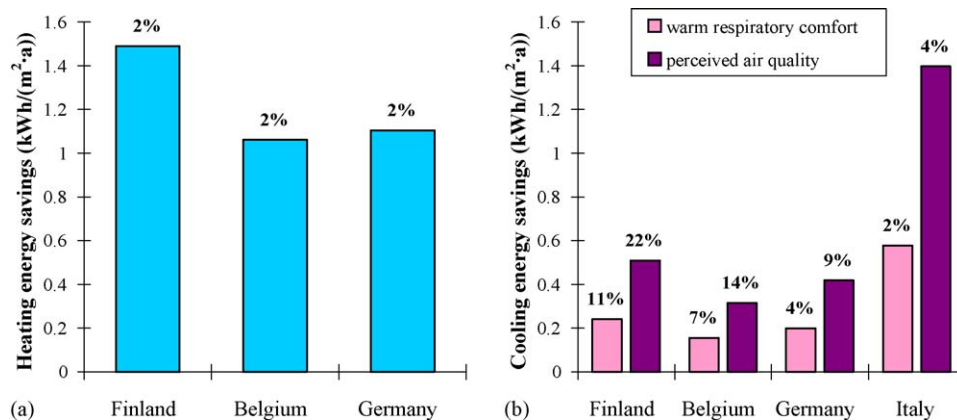


Fig. 14. Possible energy savings when the indoor temperature in the hygroscopic case is (a) decreased while maintaining the same indoor relative humidity as in the non-hygroscopic case, and (b) increased while maintaining the same comfort and air quality conditions as in the non-hygroscopic case.

Table 2
Potential reductions in the total consumption (%) of heating and cooling energy when applying hygroscopic materials in buildings

	Heating	Cooling
Direct energy savings		
Optimized control of HVAC system	2–3	5–30
No control of HVAC system	0	0–20
Reduction in energy demand	0	10–30
Indirect energy savings		
Reducing ventilation rate	5	5
Changing indoor temperature	2	2–10% (comfort), 5–20% (PAQ)

5.3. Summary of potential energy savings

The approximate potential energy savings calculated by different methods is summarized in Table 2 as a percentage of the total heating or cooling energies. It is important to note that these values are estimates based on numerical results of Simonson et al. [11,12] and a few, mainly numerical, studies reported in the literature [37,39,45–47] and must be used with caution.

6. Conclusions

Based on the literature reviewed in this paper, the moisture storage capacity of hygroscopic materials during transient changes in ambient air relative humidity (moisture buffering capacity) is an important parameter that requires further research into standard test methods and facilities that can quantify it accurately and repeatably. To help with this standard development, two different test facilities are developed and presented in this paper together with a numerical model, which can be used to compare the results from these different facilities. The model can also be used to investigate other test conditions and materials and help formulate a testing standard. Since the experimental facilities and numerical model will be applied in a companion paper [1] to investigate the moisture buffering capacity of spruce plywood, the thermal and moisture transfer properties of spruce plywood are included in this paper.

Both of these facilities described in this paper are able to provide well-controlled temperature and humidity boundary conditions for the hygroscopic material being investigated and permit these boundary conditions to be changed rapidly. One facility (termed the glass jar facility) uses a hanging mass balance and small, sealed jars containing saturated salt solutions located in a controlled environmental chamber. The other facility (termed the transient moisture transfer (TMT) facility) is more complex and provides fully developed air flow above the hygroscopic material using a small scale wind tunnel connected to an environmental chamber. The glass jar facility provides more constant humidity conditions and is able to change these conditions more rapidly than the TMT facility, but is limited to investigate natural convection moisture transfer and small samples. On the other hand, the air flow and convective transfer coefficients are well controlled in the TMT

facility and are known within $\pm 10\%$. The bias uncertainty in the measurement of moisture accumulation is ± 0.4 using the glass jar facility $\pm 1.1 \text{ g/m}^2$ using the TMT facility.

The potential for hygroscopic materials to reduce energy consumption in buildings is also presented in this paper. The most promising energy savings are for buildings with mechanical cooling equipment located in hot and humid climates, but there are potential savings in all climates if the HVAC system can be optimally controlled to regulate the indoor climate, comfort and air quality. The results show that moisture transfer has the potential to reduce the energy consumption of buildings “directly” and “indirectly”. Direct savings are defined as savings in the heating and cooling of a building that result when applying hygroscopic materials. Indirect savings are defined as savings that result from adjusting the ventilation rate and indoor temperature while maintaining adequate indoor air quality and comfort with hygroscopic materials. The potential direct energy savings are small for heating (2–3% of the total heating energy), but significant for cooling (5–30% of the total cooling energy). These savings require the integration of hygroscopic materials and a well-controlled HVAC system. The potential indirect savings for heating are in the order of 5%, while they range from 5 to 20% for cooling.

Acknowledgements

The experimental test facilities presented in this paper have been developed with funding from the Canada Foundation for Innovation (CFI) and testing was funded by the Natural Sciences and Engineering Research Council of Canada (NSERC) Discovery Grant program and Special Research Opportunities program. The energy impact study was funded by Wood Focus Oy. The financial assistance of CFI, NSERC and Wood Focus are greatly appreciated.

References

- [1] O.F. Osanyintola, P. Talukdar, C.J. Simonson, Effect of initial conditions, boundary conditions and thickness on the moisture buffering capacity of spruce plywood, *Energy and Buildings* 38 (10) (2006) 1283–1292.
- [2] J. Toftum, A.S. Jorgensen, P.O. Fanger, Upper limits of air humidity for preventing warm respiratory discomfort, *Energy and Buildings* 28 (1998) 15–23.
- [3] J. Toftum, A.S. Jorgensen, P.O. Fanger, Upper limits for indoor air humidity to avoid uncomfortably humid skin, *Energy and Buildings* 28 (1998) 1–13.
- [4] L. Fang, G. Clausen, P.O. Fanger, Impact of temperature and humidity on the perception of indoor air quality, *Indoor Air* 8 (1998) 80–90.
- [5] N. Mendes, F.C. Winkelmann, R. Lamberts, P.C. Philippi, Moisture effects on conduction loads, *Energy and Buildings* 35 (2003) 631–644.
- [6] F. Lucas, L. Adelard, F. Garde, H. Boyer, Study of moisture in buildings for hot humid climates, *Energy and Buildings* 34 (2002) 345–355.
- [7] S. Aththajariyakul, T. Leephakpreeda, Real-time determination of optimal indoor-air condition for thermal comfort, air quality and efficient energy usage, upper limits for indoor air humidity to avoid uncomfortably humid skin, *Energy and Buildings* 36 (7) (2004) 720–733.
- [8] C. Crawford, P. Manfield, A. McRobie, Assessing the thermal performance of an emergency shelter system, *Energy and Buildings* 37 (5) (2005) 471–483.

- [9] J. Arias, P. Lundqvist, Heat recovery and floating condensing in supermarkets, *Energy and Buildings* 38 (2) (2006) 73–81.
- [10] D. Yu, S.A. Klein, D.T. Reindl, An evaluation of silica gel for humidity control in display cases, *WAAC Newsletter* 23 (2.) (2001).
- [11] C.J. Simonson, M. Salonvaara, T. Ojanen, Improving indoor climate and comfort with wooden structures, *VTT Building Technology*, Espoo: VTT Publications 431, <http://virtual.vtt.fi/inf/publications/2001/P431.pdf>, VTT Building and Transport, 2001.
- [12] C.J. Simonson, M. Salonvaara, T. Ojanen, Moderating indoor conditions with hygroscopic building materials and outdoor ventilation, *ASHRAE Transactions* 110 (2) (2004) 804–819.
- [13] C.J. Simonson, S.O. Olutimayin, M. Salonvaara, T. Ojanen, J. O'Connor, Potential for hygroscopic building materials to improve indoor comfort and air quality in the Canadian climate, in: *Proceedings (CD) of the Performance of the Exterior Envelopes of Whole Buildings IX International Conference*, Clearwater Beach, FL, December 5–10, 2004, 15 pp.
- [14] C.J. Simonson, M. Salonvaara, T. Ojanen, Heat and mass transfer between indoor air and a permeable and hygroscopic building envelope. Part I. Field measurements, *Journal of Thermal Envelope and Building Science* 28 (1) (2004) 63–101.
- [15] A.H. Holm, H.M. Kunzel, K. Sedlbauer, Predicting indoor temperature and humidity conditions including hygrothermal interactions with the building envelope, *ASHRAE Transactions* 110 (2) (2004) 820–826.
- [16] C. Rode, T. Mitamura, J. Shultz, T. Padfield, Test cell measurements of moisture buffer effects, in: *Proceedings of the Sixth Nordic Building Physics Symposium*, Trondheim, Norway, (2002), pp. 619–626.
- [17] R. Peukhuri, C. Rode, K.K. Hansen, Moisture buffering capacity of different insulation materials, in: *Proceedings (CD) of the Performance of Exterior Envelopes of Whole Buildings IX International Conference*, Clearwater Beach, FL, USA, 2004, 14 pp.
- [18] M. Salonvaara, T. Ojanen, A. Holm, H.M. Kunzel, A.N. Karagiozis, Moisture buffering effects on indoor air quality—experimental and simulation results, in: *Proceedings (CD) of the Performance of Exterior Envelopes of Whole Buildings IX International Conference*, Clearwater Beach, FL, 2004, 11 pp.
- [19] K. Svennberg, L. Hedegaard, C. Rode, Moisture buffer performance of a fully furnished room, in: *Proceedings (CD) of the Performance of Exterior Envelopes of Whole Buildings IX International Conference*, Clearwater Beach, FL, 2004, 11 pp.
- [20] S. Hameury, Moisture buffering capacity of heavy timber structures directly exposed to an indoor climate: a numerical study, *Buildings and Environment* 40 (2005) 1400–1412.
- [21] C.J. Simonson, Energy consumption and ventilation performance of a naturally ventilated ecological house in a cold climate, *Energy and Buildings* 37 (1) (2005) 23–35.
- [22] J. Liu, Y. Aizawa, H. Yoshino, Experimental and numerical study on indoor temperature and humidity with free water surface, *Energy and Buildings* 37 (4) (2005) 383–388.
- [23] S. Hameury, T. Lundstrom, Contribution of indoor exposed massive wood to a good indoor climate: in situ measurement campaign, *Energy and Buildings* 36 (2004) 281–292.
- [24] S. Olutimayin, C.J. Simonson, Measuring and modeling vapor boundary layer growth during transient diffusion heat and moisture transfer in cellulose insulation, *International Journal of Heat and Mass Transfer* 48 (2005) 3319–3330.
- [25] C. Rode, A. Holm, T. Padfield, A review of humidity buffering in the interior spaces, *Journal of Thermal Envelope and Building Science* 27 (3) (2004) 221–226.
- [26] C. Rode, R. Peukhuri, K.K. Hansen, B. Time, K. Svennberg, J. Arfvidsson, T. Ojanen, Moisture buffer value of materials in buildings, in: *Proceedings of the Nordic Building Physics Conference vol. 1*, Reykjavik, Iceland, June 13–15, 2005, pp. 108–115.
- [27] JIS A 1470-1. Test method of adsorption/desorption efficiency for building materials to regulate an indoor humidity-Part 1: Response method of humidity, Japanese Standards Association, Tokyo, 2002.
- [28] D.J. Gardner, The relevance of surface properties & wood finishes to the wood science & technology research community, in: *Proceedings of the Second SWST Annual Fundamental Disciplines Session*, 2004 <http://www.swst.org/meetings/AM04/Gardner.pdf>.
- [29] ISO, Measurement of fluid flow by means of pressure differential devices, ISO 5176-1, Switzerland, 1991.
- [30] M. Kaviany, *Principles of Heat Transfer in Porous Media*, Springer-Verlag, New York, 1991.
- [31] H.M. Kuenzel, Simultaneous Heat and Moisture Transport in Building Components—One- and Two-dimensional Calculation using Simple Parameters, IRB Verlag, Fraunhofer-Informationszentrum Raum and Bau, Stuttgart, Germany, 1995.
- [32] O.F. Osanyintola, Transient moisture characteristics of spruce plywood, M.Sc. Thesis, Department of Mechanical Engineering, University of Saskatchewan, 2005, <http://library.usask.ca/theses/available/etd-12222005-082100/>.
- [33] L. Wadso, K. Svennberg, A. Dueck, An experimentally simple method for measuring sorption isotherms, *Drying Technology* 22 (10) (2004) 2427–2440.
- [34] ASTM, Standard test method for steady-state heat flux measurement and thermal transmission properties by means of the heat flow meter apparatus, ASTM C 518, Philadelphia, 2003.
- [35] ASTM, Standard test method for water vapor transmission of materials, ASTM E96/E96M, Philadelphia, 2005.
- [36] C.J. Simonson, M. Salonvaara, T. Ojanen, The effect of structures on indoor humidity—possibility to improve comfort and perceived air quality, *Indoor Air* 12 (2002) 243–251.
- [37] L. Fang, P. Wargocki, T. Witterseh, G. Clausen, P.O. Fanger, Field study on the impact of temperature, humidity and ventilation on perceived air quality, in: *Proceedings of the Indoor Air'99*, vol. 2, Edinburgh, (1999), pp. 107–112.
- [38] CEN, Ventilation for buildings—design criteria for the indoor environment, European Committee for Standardization, Report CR 1752, 1988.
- [39] P.W. Fahey, A.A. Kerestecioglu, Dynamic modeling of combined thermal and moisture transport in buildings: effect on cooling loads and space conditions, *ASHRAE Transactions* 91 (2A) (1985) 461–472.
- [40] K. Keeney, J.E. Braun, A simplified method for determining optimal cooling control strategies for thermal storage in building mass, *International Journal of HVAC&R Research* 2 (1) (1996) 59–78.
- [41] I. Andresen, M.J. Brandemuehl, Heat storage in building thermal mass—a parametric study, *ASHRAE Transactions* 98 (1) (1992) 910–918.
- [42] J.E. Braun, Reducing energy costs and peak electrical demand through optimal control of building thermal storage, *ASHRAE Transactions* 96 (2) (1990) 876–888.
- [43] ASHRAE, Thermal environmental conditions for human occupancy, ANSI/ASHRAE Standard 55, Atlanta, 2004.
- [44] J. Sundell, What we know, and what don't know about sick building syndrome, *ASHRAE Journal* 38 (6) (1996) 51–57.
- [45] O. Seppänen, Estimated cost of indoor climate in Finnish buildings, in: *Proceedings of the Indoor Air'99*, vol. 4, Edinburgh, (1999), pp. 13–18.
- [46] M. Liu, Y. Zhu, B.Y. Park, D.E. Claridge, D.K. Feary, Airflow reduction to improve building comfort and reduce energy consumption—a case study, *ASHRAE Transactions* 105 (1) (1999) 384–390.
- [47] M. Woloszyn, G. Rusaouën, G. Fraisse, J.-L. Hubert, Predicting indoor climate using electric analogy estimations of condensation potential, in: *Proceedings of the Healthy Buildings 2000*, vol. 3, Helsinki, (2000), pp. 165–170.
- [48] ASTM, Maintaining constant relative humidity by means of aqueous solutions, ASTM E 104, Philadelphia, 1985.